JACS
JOURNAL OF THE AMERICAN CHEMICAL SOCIETY

COMMUNICATION

pubs.acs.org/JACS

Rectification of Nanopores at Surfaces

Niya Sa and Lane A. Baker*

Department of Chemistry, Indiana University, Bloomington, Indiana 47405, United States

Supporting Information

ABSTRACT: At the nanoscale, methods to measure surface charge can prove challenging. Herein we describe a general method to report surface charge through the measurement of ion current rectification of a nanopipette brought in close proximity to a charged substrate. This method is able to discriminate between charged cationic and anionic substrates when the nanopipette is brought within distances from ten to hundreds of nanometers from the surface. Further studies of the pH dependence on the observed rectification support a surface-induced mechanism and demonstrate the ability to further discriminate between cationic and nominally uncharged surfaces. This method could find application in measurement and mapping of heterogeneous surface charges and is particularly attractive for future biological measurements, where noninvasive, noncontact probing of surface charge will prove valuable.

An interesting and well-studied phenomenon exhibited by some nanopore devices is ion current rectification.[1] In this context, rectification means that ions flow preferentially through the nanopore in one direction relative to the other. Shape (e.g., cylindrical, conical, etc.) and distribution of cationic or anionic charge present on the nanopore walls have been proven to play important roles in the extent and direction of rectification observed. Nanoscale effects, such as electrical-double layer (EDL) overlap[1a,2] or so-called "squeezing effects" of ion concentrations have been discussed as the origins of rectification.[3] Experimentally, rectification is measured by monitoring the current that flows through the nanopore under an applied transpore potential and can lead to a nonlinear diode-like current−voltage behavior. Rectification can be represented quantitatively as the ion current rectification (ICR) ratio, defined as the ratio of current passed at a potential relative to the current passed at a corresponding potential of opposite polarity. Here we report ICR ratios measured at ±1 V applied transpore potential (eq 1)

$$ICR_{ratio} = \frac{i_{(-1V)}}{i_{(+1V)}} \quad (1)$$

Common nanopore devices that exhibit ICR include polymer membranes,[4] silicon nitride nanopores,[1c] nanofluidic channels,[5] protein channels,[6] and glass nanopipettes.[1a,7] A number of reports have sought to develop nanofluidic devices that utilize the ICR effect to create fluidic diodes, chemical sensors, or platforms for separations. For instance, chemically modified nanopipettes have been reported that sense analytes such as DNA, proteins,[8] and metal cations[9] when specific binding of the analyte to the nanopore altered the nanopipette surface charge, demonstrated by changes in the measured ICR ratio.

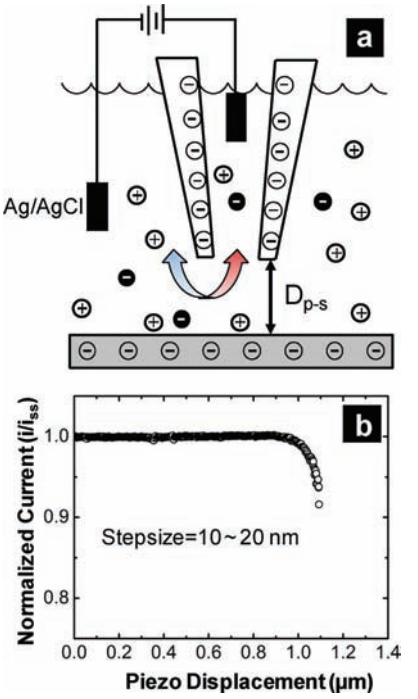

Figure 1. Measurement of ion current through nanopipettes in proximity of a substrate. (a) Schematic of experiment described. A Ag/AgCl electrode is placed inside an electrolyte-filled nanopipette. The ion current between this electrode and a second Ag/AgCl electrode in the bath solution is measured as a function of both the potential difference applied and the nanopipette position relative to a surface of interest. D_{p-s} is the probe−substrate distance. (b) Approach curve of nanopipette, in which normalized ion current as a function of piezo displacement is measured.

The aforementioned studies demonstrate the importance of surface charge on the asymmetric surface potential or ion concentration distributions and highlight the influence of the nanopipette surface chemistry on the ICR ratio. Here, we communicate asymmetric, charged nanopores (in the form of nanopipettes) that can report effects of the substrate charge through changes in the observed ICR ratio when moved in close proximity to a charged substrate. The experiment is depicted in Figure 1a. Nanopipettes were first fabricated from quartz capillaries with a CO_2 laser-based puller and characterized

Received: April 27, 2011
Published: June 15, 2011

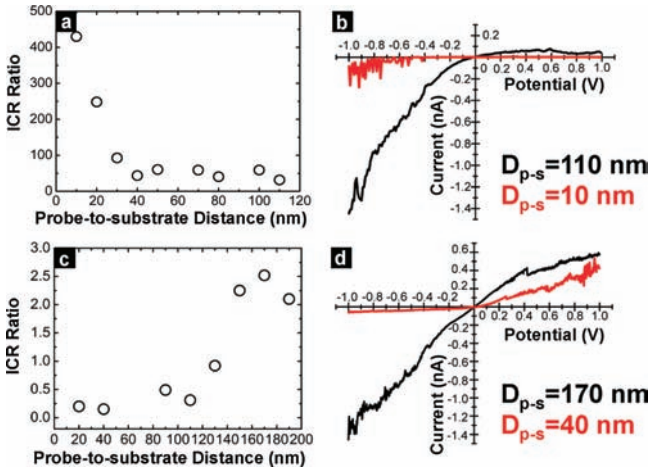

Figure 2. ICR ratio plotted as a function of nanopipette position from a substrate and illustrative current−voltage responses. (a) ICR ratio as a function of probe−substrate distance (D_{p-s}) for a nanopipette approaching an anionic ($PDMS^{OH}$) substrate. (b) Current−voltage response at probe−substrate distances of 110 nm (black) and 10 nm (red). For the anionic surface, data recorded in 50 mM KCl, 2 mM KH_2PO_4, pH 8.0. (c) ICR ratio as a function of probe-substrate distance (D_{p-s}) for a nanopipette approaching a cationic ($PDMS^{NH2}$) substrate. (d) Current−voltage response at probe−substrate distances of 170 nm (black) and 40 nm (red). For the cationic surface, data recorded in 50 mM KCl, 2 mM KH_2PO_4, pH 6.8.

electrochemically and with electron microscopies. A quartz nanopipette with anionic surface charge from pendant silanol groups was brought in close proximity to an elastomeric substrate with a piezoelectric positioner. By monitoring the steady-state ion current through the nanopipette as the nanopipette approaches a substrate, the distance from the surface can be determined.[10] Measurement of the current−voltage response of the nanopipette at discrete steps allows the influence of the substrate charge on the ICR ratio to be determined. Nanopipettes employed in this manner provide a unique platform to study fundamentals of nanofluidic phenomena and provide a tool to measure the relative cationic or anionic charge of a surface.

To address the influence of substrate charge, two elastomeric surfaces were prepared. A poly(dimethylsiloxane) substrate ($PDMS^{OH}$) was prepared from a commercial kit according to manufacturer's specifications, and the substrate was cleaned in an oxygen plasma to remove surface contamination and promote surface hydroxide formation.[11] A second PDMS substrate was chemically functionalized with (3-aminopropyl)triethoxysilane to generate a surface with pH-dependent cationic surface charge.[12] For approach of the nanopipette to a substrate, an initial measurement of the steady-state ion current for the nanopipette far removed from the surface was recorded. The nanopipette was then approached to the substrate (step size ∼10 nm) with an automated approach until the ion current decreased to 90% of its steady state value as shown in Figure 1b. The decrease observed occurs due to hindered transport of ions through the small gap (D_{p-s}) which separates the nanopipette probe and substrate surface. This indicates that the nanopipette is close to the surface; for the small-diameter nanopipettes employed here, D_{p-s} is on the order of hundreds of nanometers or less.[13] The nanopipette was then manually advanced with the current−voltage response recorded at each point in the manual approach. The potential was scanned from ±1 V at a scan rate of 0.05 V/s to ensure a steady-state response.[2,14] Eventually, no current was recorded through the nanopipette, which was regarded as the point of zero probe−substrate distance, where the nanopipette was sealed to the elastomeric surface. In some instances, no seal or zero point could be obtained, likely due to the angle of approach of the nanopipette or surface roughness, and these data were not used further in analysis.

The ICR ratios as functions of probe−substrate distance and selected current−voltage responses for approach to an anionic substrate are presented in Figure 2a and b. Both the nanopipette and the solution bathing the $PDMS^{OH}$ were filled with an electrolyte concentration of 50 mM KCl with 2 mM KH_2PO_4, pH 8.0. Previous reports have indicated that the structure of a $PDMS^{OH}$ surface resembles that of inorganic silica, with surface silanol groups that carry an anionic surface charge under alkaline conditions.[11a] For the ICR ratio−distance plot (Figure 2a), the ICR ratio stays constant for D_{p-s} greater than 40 nm. For probe−substrate distances <40 nm, significant increase of the ICR ratio with decreasing D_{p-s} is observed. The ICR ratio reaches a maximum of ∼400 when separation between probe and substrate is ∼10 nm. Representative current−voltage plots at D_{p-s} of 110 and 10 nm are shown in Figure 2b (see Supporting Information [SI] for further plots). From the current−voltage plot, the overall magnitude of the current response is lowered due to the increased access resistance of the probe−substrate gap,[15] but the currents recorded at positive values are attenuated to a greater extent. A plausible mechanism for this increase in rectification is both charge screening of chloride ions moving into the nanopipette and depletion of anions in the double layer by the anionic charge at the surface of the $PDMS^{OH}$ substrate. When considered in the context of the anionic charge of the nanopipette, the ICR effect is enhanced in close proximity to the surface relative to that of the nanopipette alone.

The ICR ratio as a function of probe−substrate distance and selected current−voltage responses for approach to a cationic substrate are presented in Figure 2c and d. An electrolyte concentration of 50 mM KCl with 2 mM KH_2PO_4, pH 6.8, was filled into both the nanopipette and the solution bathing the $PDMS^{NH2}$ substrate. In this case, the ICR ratio displays a distance-dependent response that is opposite from the anionic $PDMS^{OH}$ surface. At large probe-to-surface separation (>150 nm), the ICR ratio is ∼2.2. As the nanopipette approaches the substrate, the overall current magnitude decreases, again due to the increase in access resistance. The ICR ratio decreases rapidly for small probe−substrate separations, with values of 0.92, 0.15, and 0.20 for D_{p-s} of 130, 40, and 20 nm, respectively. We attribute this effect to a surface charge-induced depletion of local concentration of co-ions (K^+) and an enrichment of counterion (Cl^-) concentration. Therefore, the charge of the substrate is a critical factor in ion transport, as the probe−substrate gap becomes a dominant resistive element. Interestingly, a negatively charged nanopipette in close proximity to a positively charged surface mimics properties of asymmetric fluidic diodes designed by Siwy and co-workers for the case of asymmetrically charged nanopores[16] and may provide a manner to investigate such phenomena further. For instance, at some intermediate distances (see SI) current−voltage responses near zero applied potential diminished greatly, which suggests the possibility of formation of a depletion zone between the positively charged $PDMS^{NH2}$ substrate and the negatively charged nanopipette surface. To ensure the current−voltage response observed was not the result of silanes adsorbed to the nanopipette, the nanopipette was

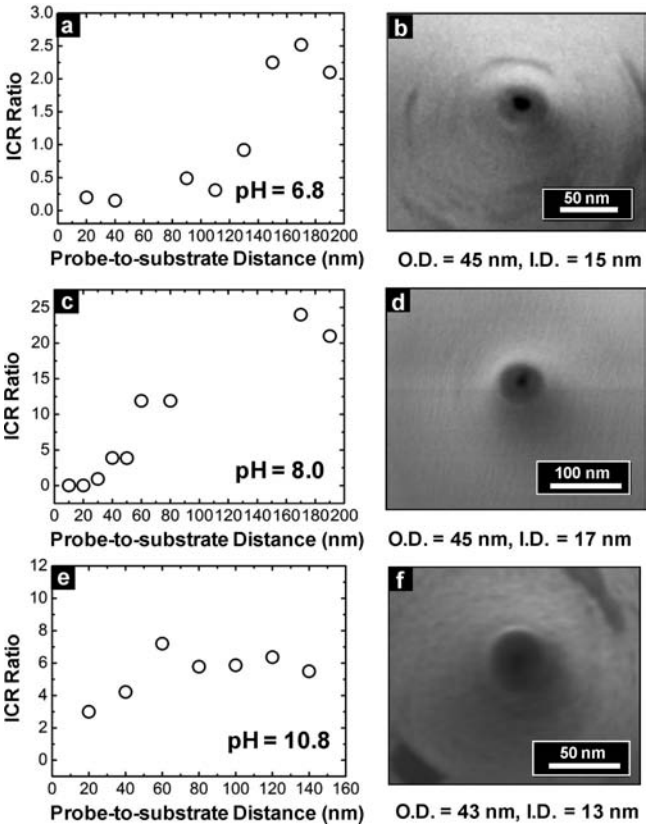

Figure 3. ICR ratio plotted as function of probe-to-surface distance when nanopipette approached $PDMS^{NH2}$ substrate at pH 6.8 (a), 8.0 (c), and 10.8 (e), with corresponding SEM images (b), (d) and (f). Electrolyte concentration was kept the same at 50 mM KCl, 2 mM KH_2PO_4. O.D. indicates outer diameter, I.D. indicates inner diameter.

withdrawn after reaching the zero point, and the current−voltage response was recorded. Results showed that the two current−voltage curves taken at large probe−substrate separation before and after the approach were very similar, which illustrates that the surface charge of the nanopipette is not significantly changed in this experiment. (see SI).

Measurement of the current−voltage response for a nanopipette approaching a $PDMS^{NH2}$ surface as a function of pH was also recorded. Panels a, c, and e of Figure 3 display the current rectification ratio plotted as a function of probe-substrate distance at pHs of 6.8, 8.0, and 10.8 respectively. Panesl b, d, and f of Figure 3 show scanning electron micrographs of nanopipettes pulled from the same capillary as those used in the measurement. At pHs 6.8 and 8.0, the ICR ratio decreased significantly with decreasing D_{p-s}. Overall, the ICR ratio changed from 2.2 to 0.2 and 21.0 to 0.02 as D_{p-s} was changed from 180 to 20 nm respectively. To minimize the cationic charge on the $PDMS^{NH2}$ substrate, a sufficiently high pH of 10.8 (as compared with isoelectric point of amine-modified surface pH 10−11) was also measured.[17] Here the ICR ratio decreased from 5.5 to 3.0 as D_{p-s} changed from 140 to 20 nm at pH 10.8, which represents a much smaller relative change and further indicates that the rectification of the nanopipette surface is still the dominant factor since the ICR ratio is larger than 1.

In summary, we have studied ion transport through nanopipettes in close proximity to charged cationic and anionic substrates. We have demonstrated experimentally that, when asymmetric charged nanopores are in close proximity to a substrate of interest, the substrate charge can play a key role in the current−voltage response observed. The recorded distance-dependent ICR ratio can thus be employed to report surface charge for the region in the vicinity of a nanopipette tip. We believe the initial results communicated here can be further extended to explore local charge densities of heterogeneous surfaces at spatial resolution on the order of the nanopipette tip diameter (<100 nm). This technique could prove valuable in studies of biological surfaces (e.g., lipid composition) and in further investigations of nanofluidic phenomena.

■ ASSOCIATED CONTENT

Supporting Information. Experimental details and current−voltage plots. This material is available free of charge via the Internet at http://pubs.acs.org.

■ AUTHOR INFORMATION

Corresponding Author
lanbaker@indiana.edu

■ ACKNOWLEDGMENT

Financial support of the National Institutes of Health, the American Heart Association and the Research Corporation (Cottrell Scholar's Award to L.A.B) are acknowledged. We thank Ms. Alicia Friedman and Ms. Chiao-Chen Chen for comments. Mr. Maksymilian A. Derylo is acknowledged for assistance with atomic force microscopy characterization.

■ REFERENCES

(1) (a) Wei, C.; Bard, A. J.; Feldberg, S. W. *Anal. Chem.* **1997**, *69*, 4627–4633. (b) Siwy, Z.; Gu, Y.; Spohr, H. A.; Baur, D.; Wolf-Reber, A.; Spohr, R.; Apel, P.; Korchev, Y. E. *Europhys. Lett.* **2002**, *60*, 349–355. (c) Cruz-Chu, E. R.; Aksimentiev, A.; Schulten, K. *J. Phys. Chem. C* **2009**, *113*, 1850–1862.

(2) White, H. S.; Bund, A. *Langmuir* **2008**, *24*, 2212–2218.

(3) (a) Tanimura, A.; Kovalenko, A.; Hirata, F. *Langmuir* **2007**, *23*, 1507–1517. (b) Han, J. Y.; Fu, J. P.; Schoch, R. B. *Lab Chip* **2008**, *8*, 23–33. (c) Davenport, M.; Rodriguez, A.; Shea, K. J.; Siwy, Z. S. *Nano Lett.* **2009**, *9*, 2125–2128.

(4) (a) Siwy, Z.; Apel, P.; Dobrev, D.; Neumann, R.; Spohr, R.; Trautmann, C.; Voss, K. *Nucl. Instrum. Methods Phys. Res., Sect. B* **2003**, *208*, 143–148. (b) Heins, E. A.; Baker, L. A.; Siwy, Z. S.; Mota, M.; Martin, C. R. *J. Phys. Chem. B* **2005**, *109*, 18400–18407. (c) Siwy, Z. S. *Adv. Funct. Mater.* **2006**, *16*, 735–746.

(5) (a) Cheng, L. J.; Guo, L. J. *ACS Nano* **2009**, *3*, 575–584. (b) Cheng, L. J.; Guo, L. J. *Chem. Soc. Rev.* **2010**, *39*, 923–938.

(6) (a) Pfaffinger, P. J.; Martin, J. M.; Hunter, D. D.; Nathanson, N. M.; Hille, B. *Nature* **1985**, *317*, 536–538. (b) Bormann, J.; Hamill, O. P.; Sakmann, B. *J. Physiol.* **1987**, *385*, 243–286. (c) Kubo, Y.; Baldwin, T. J.; Jan, Y. N.; Jan, L. Y. *Nature* **1993**, *362*, 127–133.

(7) (a) Wang, G. L.; Zhang, B.; Wayment, J. R.; Harris, J. M.; White, H. S. *J. Am. Chem. Soc.* **2006**, *128*, 7679–7686. (b) Zhang, B.; Galusha, J.; Shiozawa, P. G.; Wang, G. L.; Bergren, A. J.; Jones, R. M.; White, R. J.; Ervin, E. N.; Cauley, C. C.; White, H. S. *Anal. Chem.* **2007**, *79*, 4778–4787. (c) Umehara, S.; Pourmand, N.; Webb, C. D.; Davis, R. W.; Yasuda, K.; Karhanek, M. *Nano Lett.* **2006**, *6*, 2486–2492.

(8) (a) Umehara, S.; Karhanek, M.; Davis, R. W.; Pourmand, N. *Proc. Natl. Acad. Sci. U.S.A.* **2009**, *106*, 4611–4616. (b) Fu, Y. Q.; Tokuhisa, H.; Baker, L. A. *Chem. Commun.* **2009**, 4877–4879. (c) Actis, P.; Mak, A.; Pourmand, N. *Bioanal. Rev.* **2010**, *1*, 177–185.

(9) (a) Sa, N. Y.; Fu, Y. Q.; Baker, L. A. *Anal. Chem.* **2010**, *82*, 9963–9966. (b) Actis, P.; Vilozny, B.; Seger, R. A.; Li, X.; Jejelowo, O.; Rinaudo, M.; Pourmand, N. *Langmuir* **2011**, 6528–6533.

(10) Elsamadisi, P.; Wang, Y. X.; Velmurugan, J.; Mirkin, M. V. *Anal. Chem.* **2011**, *83*, 671–673.

(11) (a) Fakes, D. W.; Davies, M. C.; Brown, A.; Newton, J. M. *Surf. Interface Anal.* **1988**, *13*, 233–236. (b) Morra, M.; Occhiello, E.; Marola, R.; Garbassi, F.; Humphrey, P.; Johnson, D. *J. Colloid Interface Sci.* **1990**, *137*, 11–24.

(12) Li, H.; Zhang, J.; Zhou, X.; Lu, G.; Yin, Z.; Li, G.; Wu, T.; Boey, F.; Venkatraman, S. S.; Zhang, H. *Langmuir* **2010**, *26*, 5603–5609.

(13) Korchev, Y. E.; Bashford, C. L.; Milovanovic, M.; Vodyanoy, I.; Lab, M. J. *Biophys. J.* **1997**, *73*, 653–658.

(14) Guerrette, J. P.; Zhang, B. *J. Am. Chem. Soc.* **2010**, *132*, 17088–17091.

(15) Shevchuik, A. I.; Frolenkov, G. I.; Sanchez, D.; James, P. S.; Freedman, N.; Lab, M. J.; Jones, R.; Klenerman, D.; Korchev, Y. E. *Angew. Chem., Int. Ed.* **2006**, *45*, 2212–2216.

(16) (a) Daiguji, H.; Oka, Y.; Shirono, K. *Nano Lett.* **2005**, *5*, 2274–2280. (b) Kalman, E. B.; Vlassiouk, I.; Siwy, Z. S. *Adv. Mater.* **2008**, *20*, 293–297. (c) Vlassiouk, I.; Smirnov, S.; Siwy, Z. *ACS Nano* **2008**, *2*, 1589–1602. (d) Nguyen, G.; Vlassiouk, I.; Siwy, Z. S. *Nanotechnology* **2010**, *21*, 265301.

(17) (a) Yokoi, T.; Yoshitake, H.; Yamada, T.; Kubota, Y.; Tatsumi, T. *J. Mater. Chem.* **2006**, *16*, 1125–1135. (b) Chauhan, A. K.; Aswal, D. K.; Koiry, S. P.; Gupta, S. K.; Yakhmi, J. V.; Surgers, C.; Guerin, D.; Lenfant, S.; Vuillaume, D. *Appl. Phys. A* **2008**, *90*, 581–589.